STRUCTURAL SCIENCE
CRYSTAL ENGINEERING
MATERIALS

Volume 71 (2015)

Supporting information for article:

Crystal structure of magnesium dichloride decahydrate determined by X-ray and neutron diffraction under high pressure

Kazuki Komatsu, Ayako Shinozaki, Shinichi Machida, Takuto Matsubayashi, Mao Watanabe, Hiroyuki Kagi, Asami Sano-Furukawa and Takanori Hattori

S1. Pulse shape of the PLANET beamline used in the Rietveld Analysis

Coupled, unpoisoned decoupled, and poisoned decoupled moderators ranging from high intensity–low resolution to low intensity–high resolution exist in the MLF, J-PARC. The PLANET beamline is equipped with the unpoisoned decoupled moderator, which displays medium intensity and resolution, and is dedicated to studies on both powder (crystal) and amorphous materials (e.g., Arima *et al.*, 2010; Hattori *et al.*, 2015). The profile function in the Rietveld refinements may be described as a convolution of 1) the neutron pulse shape from the moderator, 2) the dispersion of the incident/diffracted beam and the positional uncertainty in detectors, and 3) sample broadening resulting from crystallite size and strain. Second and third contributions may be approximated as symmetric pseudo-Voigt functions. On the other hand, the pulse shape is defined as a convolution of the modified Ikeda–Carpenter function and a linear combination of a δ-function and an exponential decay (Tamura *et al.*, 2003). Although this function may be the most physically suitable representation of pulse shape, it is currently not implemented in any Rietveld analysis software. Alternatively, the GSAS TOF profile function 3 (Larson & Von Dreele, 2004) is widely used as a *tof* profile function in many programs in addition to GSAS. This function is a convolution of back-to-back exponential ($E(\Delta T)$) and pseudo-Voigt functions ($P(\Delta T)$). As a result, by adopting this profile function, users implicitly assume that the pulse shape from the moderator is represented by $E(\Delta T)$ and a part of $P(\Delta T)$. This assumption was made in this study to select the GSAS TOF profile function 1 ($H(\Delta T)$; Von Dreele et al., 1982) as a pulse shape function for the moderator of PLANET beamline. The GSAS TOF profile function 1 presents a similar formulation to profile function 3 but without a Lorentzian component. Therefore, it is written as a convolution of $E(\Delta T)$ and a Gaussian function ($G(\Delta T)$):

$$H(\Delta T) = G(\Delta T) \otimes E(\Delta T),$$

$$= N[e^{u}\mathrm{erfc}(y) + e^{v}\mathrm{erfc}(z)],$$

where

$$N = \frac{\alpha\beta}{2(\alpha+\beta)},$$

$$u = \frac{\alpha}{2}(\alpha\sigma^2 + 2\Delta T),$$

$$y = \frac{\alpha\sigma^2 + \Delta T}{\sqrt{2\sigma^2}},$$

$$v = \frac{\beta}{2}(\beta\sigma^2 - 2\Delta T),$$

$$z = \frac{\beta\sigma^2 - \Delta T}{\sqrt{2\sigma^2}}.$$

For the representation of the pulse shape, ΔT is simply defined using a peak center of profile (t_c), i.e.,

$$\Delta T = t - t_c,$$

instead of the peak center of Bragg peaks in the original definition in GSAS.

The profile function coefficients α, β, σ^2, and t_c are determined by the nonlinear least squares method using the pulse shape profile as a function of time (t) provided on the J-PARC website (http://j-parc.jp/researcher/MatLife/en/instrumentation/ns3.html). Representative fitting results are shown in Fig. S1, and the wavelength dependences of profile function coefficients at d-spacing corresponding to $2\theta = 90°$ are shown in Fig. S2. The fitting was unstable when α surpassed ca. 10 because the exponential term was too sharp and did not affect the profile function. The d-dependences of α, β, and t_c are empirically described using equations shown in Fig. S2. These coefficients as a function of d-spacing were tabulated in the instrument file in GSAS and considered as sample-independent parameters in the Rietveld refinement.

The GSAS TOF profile function 1 did not strictly coincide with the pulse shape (Fig. S1), in particular for the high-d region, though this may not severely affect the structure refinement results in this study. This function may be replaced by more appropriate profile functions in the future for more precise structure analysis.

S2. Intensity correction for neutron diffraction data

The intensity obtained from the sample in the cell (I_S) was subtracted by the intensity of the empty cell (I_E), normalized by the attenuation factor (A_S), and then divided by the attenuation (A_V) corrected intensity for vanadium pellet in the cell (I_V), which was also subtracted by the intensity of the empty cell:

$$I_{\text{corrected}} = \frac{A_S^{-1}(I_S - I_E)}{A_V^{-1}(I_V - I_E)}.$$

All intensities were normalized by the number of protons hitting the target (corresponding to the total incident intensity). Here, the incoherent scattering of vanadium was assumed isotropic in terms of both scattering angle and wavelength, as frequently adopted. Although this assumption is not always true and a few percent of anisotropy may be found in the current setup (e.g., Mayers, 1984), the anisotropy of vanadium scattering was not corrected to avoid complexity because it may affect our results to a small extent. Moreover, the so-called Paalman–Pings coefficient ($A_{C,\,S+C}/A_{C,C}$; see details in Paalman and Pings, 1962), which is often used as an adjustment parameter for the intensity of the

empty cell, was assumed to equal 1 because the radial collimator may mostly eliminate scattering from the cell. Attenuation factors A_S and A_V for sample and vanadium pellets, respectively, were derived from attenuation coefficients ($\mu_S(\lambda)$ and $\mu_V(\lambda)$) and geometrically calculated flight paths for incident ($t_{inc,i}$) and scattered ($t_{sca,\,i}$) neutrons for a point, p_i, in the sample pellet as follows:

$$A(\lambda) = \frac{1}{\sum_i w_i} \sum_i w_i \exp[-\mu(\lambda)(t_{inc,i} + t_{sca,i})],$$

where w_i is the weight for the point p_i derived using a Gauss–Legendre quadrature. The calculated $A(\lambda)$ was converted to $A(tof')$ for each pixel of the detector, where tof' is the time-of-flight multiplied by a convergence factor related to the data acquired at $2\theta = 90°$.

$$tof' = \frac{L_j \sin\theta_j}{L_{90} \sin\left(\frac{\pi}{4}\right)}\, tof,$$

where L_j is the total flight path, θ_j is a half of the scattering angle for j^{th} pixel, L_{90} is for the total flight path from the moderator to a pixel at $2\theta = 90°$ (L_{90} = 26.5 m), and tof is derived from the wavelength using the de Broglie relationship. Finally, for all pixels, $A(tof')$ values were merged into an one-dimensional histogram. Because I_V was corrected for sample or vanadium pellet in the cell, attenuation factors for cell components are intrinsically taken into account. Observed I_S, I_V, and I_E values are shown in Fig. S3, along with calculated A_S and A_V.

S3. Rietveld refinement results for $MgCl_2 \cdot 10H_2O$

Table S1 Experimental details of structure refinement for $MgCl_2 \cdot 10H_2O$.

	$MgCl_2 \cdot 10H_2O$
Chemical formula	$MgCl_2 \cdot 10H_2O$
M_r	275.36
Crystal system, space group	Monoclinic, *C*2/*m*
Temperature (K)	300
Pressure (GPa)	2.11
a, *b*, *c* (Å)	10.3760 (3), 7.4867 (3), 7.7273 (3)
β (°)	116.322 (2)
V (Å^3)	538.03 (2)
Z	2
Radiation type	Synchrotron x-ray, λ = 0.6133 Å
Diffractometer	PF-18C, KEK
Specimen mounting	Diamond anvil cell with cryostat
2θ values (°)	$2\theta_{min}$ = 5.0 $2\theta_{max}$ = 29.53 $2\theta_{step}$ = 0.01
R factors and goodness of fit	R_p = 0.041, R_{wp} = 0.071, R_{exp} = 0.079, $R(F^2)$ = 0.11673, χ^2 = 0.810
No. of data points	2454
No. of parameters	27

Computer program: *GSAS*.

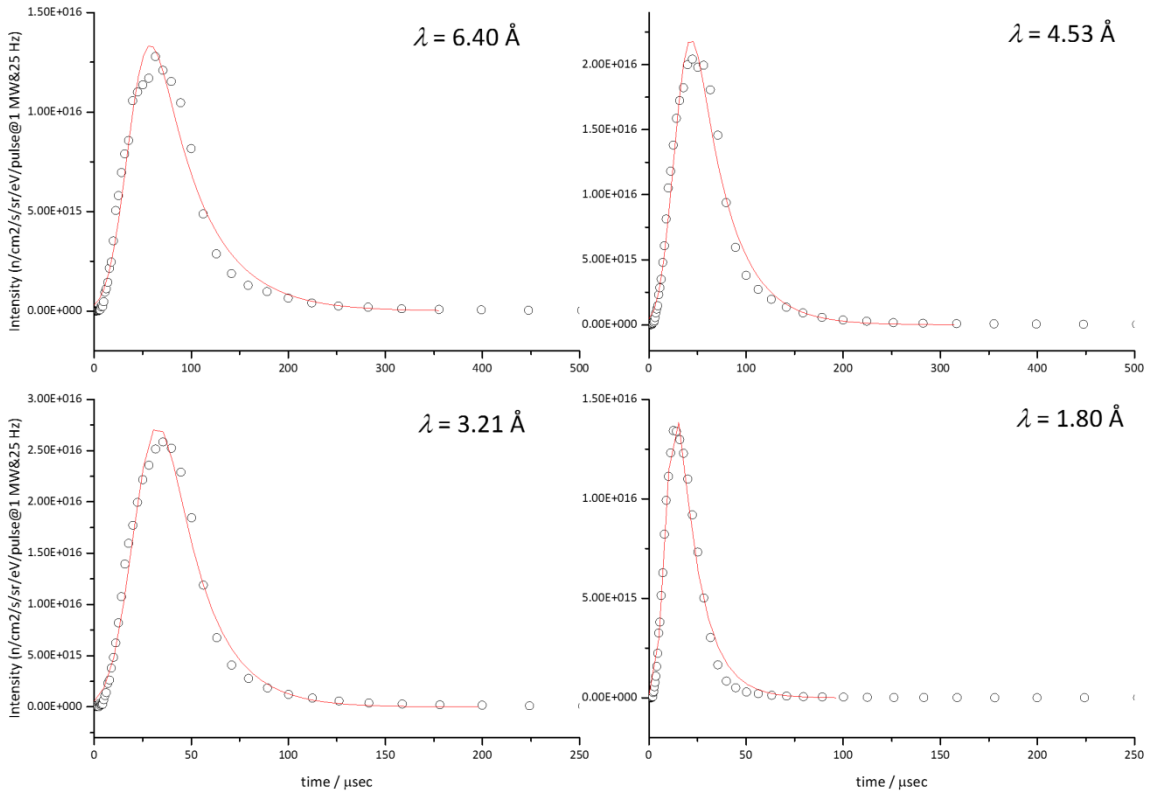

Figure S1 Representative fitting results for the pulse shape of the PLANET beamline as a function of time using the GSAS TOF profile function 1.

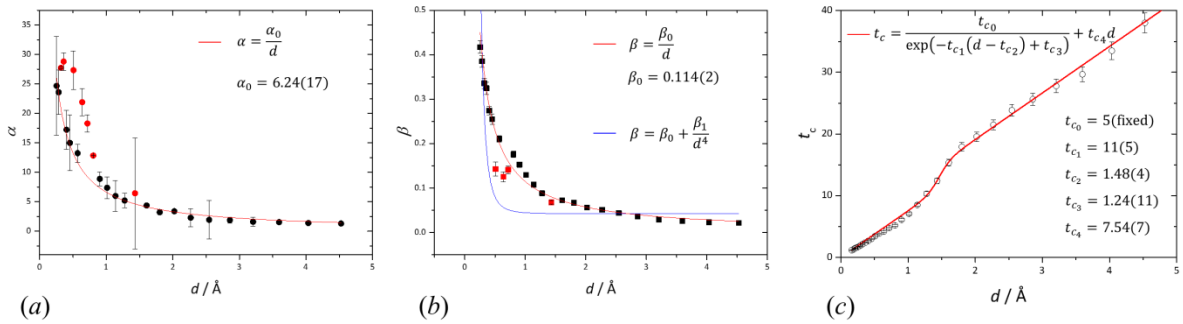

Figure S2 Fitted profile coefficients (a) α, (b) β, and (c) t_c. The d-dependences were fitted by equations shown in the respective plots. The d-dependence of β was also fitted by a different equation (blue line) generally used in the GSAS TOF profile function 3, showing inconsistency. Red points in (a) and (b) were omitted in the fitting for d-dependence due to the mismatch to other points.

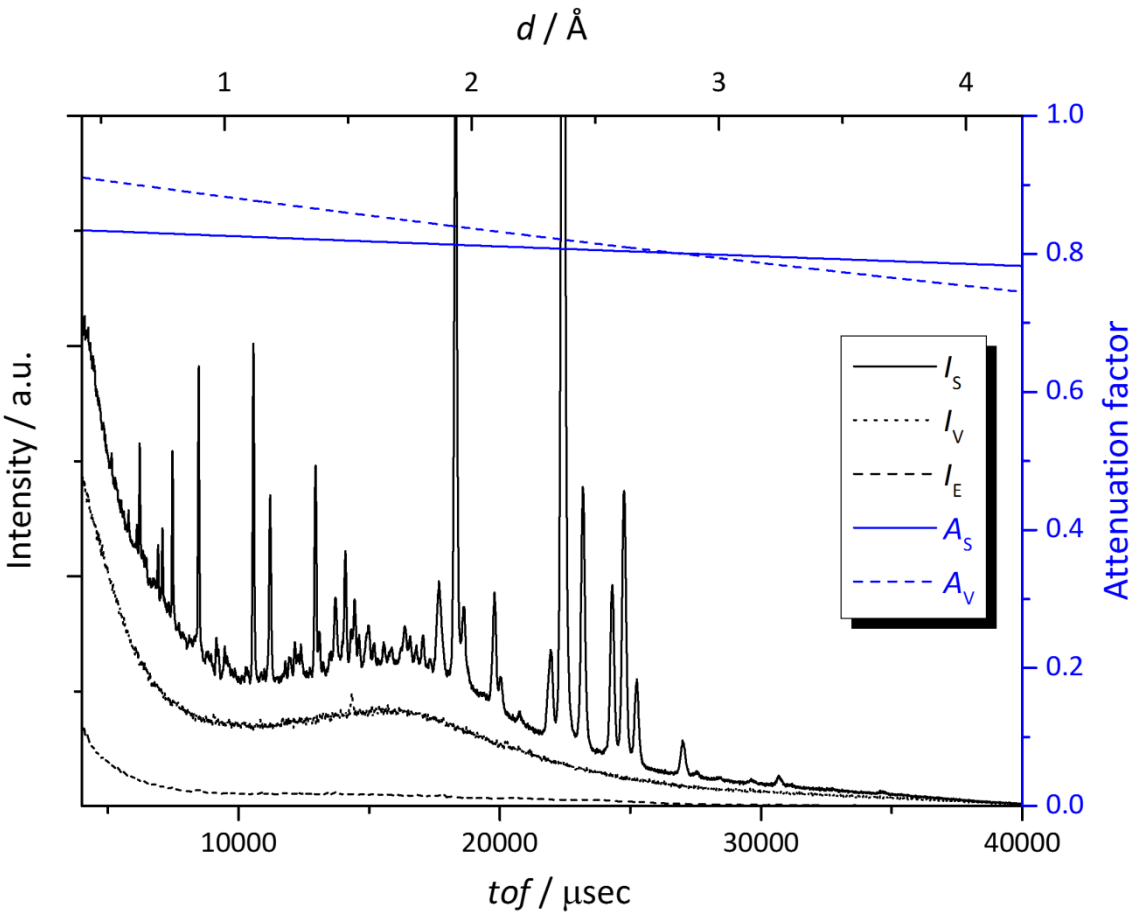

Figure S3 Intensities of sample (I_S), vanadium (I_V), and empty cell (I_E) and attenuation factors for sample (A_S) and vanadium (A_V) as functions of converged *tof* (*tof'*). Corresponding *d*-spacings are shown on the upper axis.

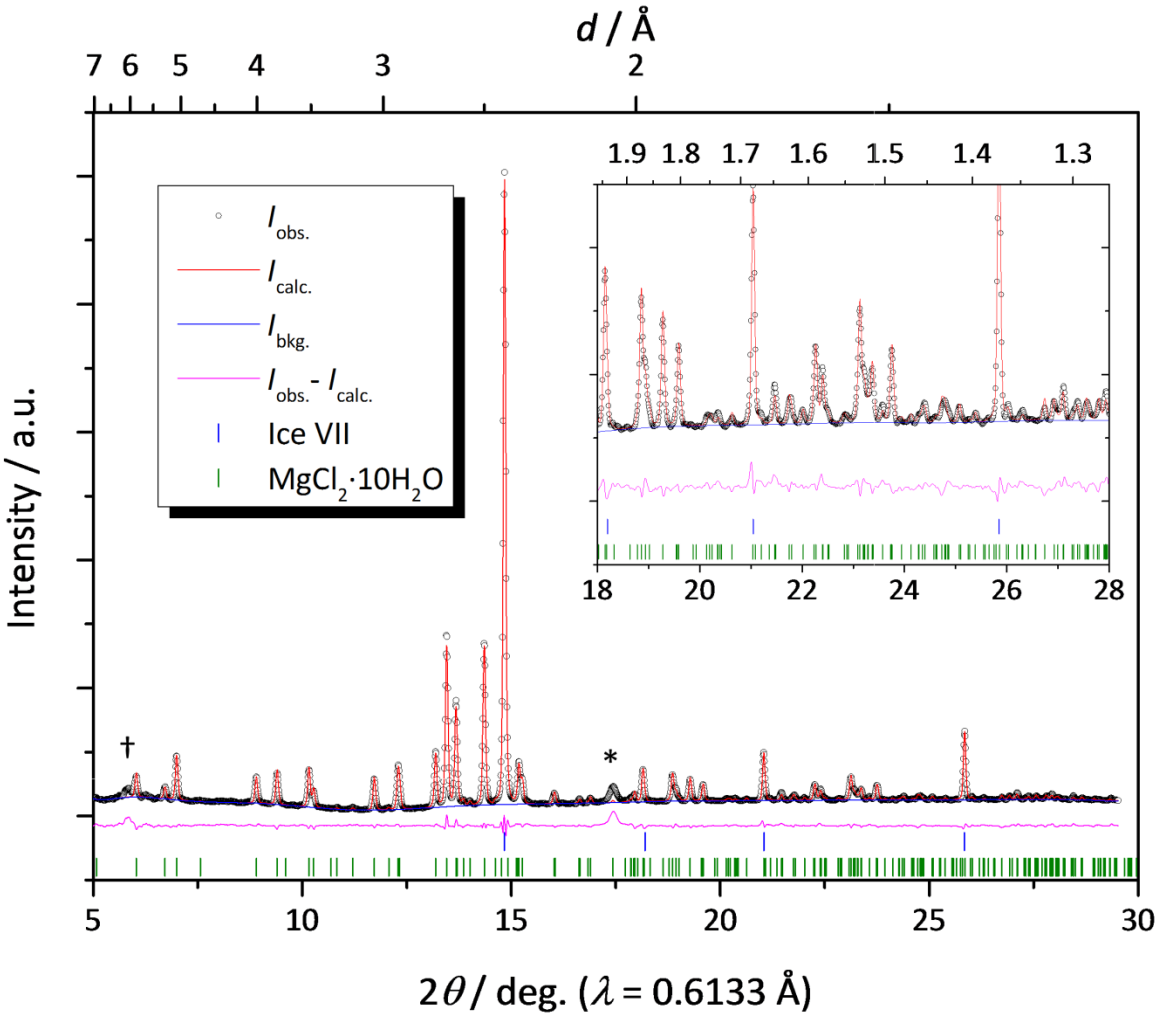

Figure S4 Rietveld fitting of $MgCl_2 \cdot 10H_2O$. The horizontal axis represents 2θ (lower) or d (upper). The inset shows an enlargement for high 2θ values. Dagger and asterisk mark parasitic scatterings from the vacuum chamber window film and the gasket material, respectively.

References

Arima, H., Hattori, T., Komatsu, K., Abe, J., Utsumi, W., Kagi, H., Suzuki, A., Suzuya, K., Kamiyama, T., Arai, M. & Yagi, T. (2010). *Journal of Physics: Conference Series* **215**, 012025.

Hattori, T.,, Sano-Furukawa, A., Arima, H., Komatsu, K., Yamada, A., Inamura, Y., Nakatani, T., Seto, Y., Nagai, T., Utsumi, W., Iitaka, T., Kagi, H., Yagi, T., Katayama, Y., Inoue, T., Otomo, T., Suzuya, K. & Arai, M. (2015) *in preparation*.

Larson, A. & Von Dreele, R. (2004). *Los Alamos National Laboratory, Report LAUR-86-748*.

Mayers, J. (1984). *Nuclear Instruments and Methods in Physics Research* **221**, 609-618.

Paalman, H. H. & Pings, C. J. (1962). *Journal of Applied Physics* **33**, 2635-2639.

Tamura, I., Maekawa, F., Harada, M., Arai, M., Aizawa, K., Soyama, K. & Shibata, K. (2003). Report JAERI-RESEARCH--2003-008.

Von Dreele, R. B., Jorgensen, J. D. & Windsor, C. G. (1982). *Journal of Applied Crystallography* **15**, 581-589.